*Journal of Geosciences and Geomatics, 2017, Vol. 5, No. 3, 96-108*
Available online at http://pubs.sciepub.com/jgg/5/3/1

DOI:10.12691/jgg-5-3-1

# Appraisal of Methods for Estimating Orthometric Heights – A Case Study in a Mine

**M. S. Peprah[1,*], S. A. Kumi[2]**

[1]Department of Geomatic Engineering, University of Mines and Technology, Tarkwa-Western Region, Ghana
[2]Department of Geological Engineering, University of Mines and Technology, Tarkwa-Western Region, Ghana
*Corresponding author: michaelstanleypeprah@ymail.com

**Abstract** The concept of orthometric heights system determination plays a major key role in geodesy, and it has broad applications in various fields and activities. In geodesy, one significant quantity is the orthometric height, the height above or below the geoid along the gravity plumbline. Conventionally, the orthometric height is determined by gravimetry and levelling techniques. However, the aforementioned techniques has its own demerits. Thus, the error is accumulated with the increase of the propagation measurement line, it is difficult to convert two separated points which is located in two continents or islands separated by sea. These techniques are tedious, time consuming and expensive. In order to resolve this challenge, many researchers resort to various techniques and approaches of obtaining orthometric heights for an area using various mathematical models. It is in this quest that, this study seek to estimate orthometric heights of a mine by utilizing plausible alternative techniques based on artificial neural networks (ANN), multivariate adaptive regression splines (MARS), polynomial regression models and multiple linear regression (MLR). The working efficiency and performance of each model has been assessed based on statistical indicators of Mean (M), Mean Square Error (MSE), Root Mean Square Error (RMSE), Mean Bias Error (MBE), Mean Absolute Error (MAE), Standard Deviation (SD), Correlation coefficient (R), Correction of determination ($R^2$), and Signal to Noise Ratio (SNR). The statistical findings reveal that all the models produce satisfactory results in estimating the orthometric heights in the mine. MARS and ANN models compare to the MLR and polynomial models achieved higher results in terms of accuracy with mean and standard deviation of -0.000001888 m, +2.24736 m, and +0.005835 m and 0.095063 m respectively. This study will create the opportunity for geospatial practitioners to recognize the significant of ANN, MARS, MLR, and Polynomial model in solving some of the problems in geoscientific community.

***Keywords:*** *orthometric heights, geoid, ellipsoid, multivariate adaptive regression splines, vertical coordinates, artificial neural network, multiple linear regression, polynomial mathematical model, ordinary least square, total least square*

**Cite This Article:** M. S. Peprah, and S. A. Kumi, “Appraisal of Methods for Estimating Orthometric Heights – A Case Study in a Mine.” *Journal of Geosciences and Geomatics*, vol. 5, no. 3 (2017): 96-108. doi: 10.12691/jgg-5-3-1.

## 1. Introduction

The orthometric height is the distance, measured positive outwards or negative inwards along the plumbline, from the geoid (zero orthometric height) to a point of interest, usually on the topographic surface [1,2]. The curved plumbline is at every point tangential to the gravity vector generated by the Earth, its atmosphere and rotation. The Orthometric height can be computed from the geopotential number if available, using the mean value of the Earth’s gravity acceleration along the plumbline between the geoid and the Earth’s surface [3]. Alternatively and more practically, it can be computed from spirit levelling measurements using the so-called orthometric correction, embedded in which is the mean value of gravity [4]. Ignoring levelling errors and the many issues, surrounding practical vertical datum definition [5,6], the rigorous determination of the orthometric height reduces to the accurate determination of the mean value of the Earth’s gravity acceleration along the plumbline between the geoid and the point of interest.

An approximate method for the evaluation of the mean gravity has been discussed for more than a century. The first theoretical attempt is attributed to [7]. In Helmert’s definition of the orthometric height, the Poincare-Prey gravity gradient is used to evaluate the approximate value of mean gravity from the gravity observed on the Earth’s surface [1,2]. Later, [8] and [9] took into account the mean value of the gravimetric terrain correction within the topography. [1] also mentioned a general method for calculating mean gravity along the plumbline that includes the accounting for the shape of the terrain. More recently, [10,11,12] introduced further corrections due to vertical and lateral variations in the topographical mass-density. In addition to the above theoretical developments, numerous empirical studies have been published on the Orthometric height determination [13-21].

In Geodetic surveys, defining a system of heights consists of choosing a reference surface, adopting a definition with physical or geometrical significance, whereby the position of the surface of the Earth is described as against the reference surface [22]. The level surfaces are not parallel, the system of orthometric heights is defined as that system in which the geoid is the reference surface and the orthometric height is the force line segment included between the position of the point on the surface of the Earth and the geoid respectively. In most cases geodesists are interested in the orthometric height as being the measured one family of surfaces, identified as geoid. The surface of the geoid is one of a whole family of surfaces or equipotential leads of the gravity field of the Earth. Most geodesic measurements, by virtue of their connection with the local reference plane, are influenced by the gravity field of the Earth. The local surfaces, as their name indicate, are surfaces with constant gravitational potential [23].

The gravity vector, or the direction of the vertical of any point is perpendicular to this level surface passing through that point. The Orthometric height has a more physical meaning than the geometrical one of the ellipsoidal height [24]. The orthometric height was traditionally determined, by levelling techniques whereby height increases were obtained by intersecting the line of sight of a levelling instrument tangentially on the level surface, on two gradual levelling staff. Knowing the orthometric height is necessary for accurate engineering operations such as dams, pipes, tunnels, which operate with fluids and their flow. During the last century it was admitted that the average surface of the ocean was a good approximation of the level surface of the gravity field of the Earth and this surface was chosen as the references surface for heights. These geoid became a concept very used in practical determination of the Orthometric heights and widely such as heights above the average sea level or heights above the geoid are considered equivalent in the contest of most measuring applications [25].

It seems that not only the traditional geodesic measuring and photogrammetry methods are decisively influenced by GPS possibilities but also physical geodesy within the determination of orthometric heights, which is closely connected as it is known to the definition of the geoid as a reference surface. An understanding of heights is essential to the study of any field of Geomatic orthometric height [26]. Geometrically, is the length of a (curved) plumbline interesting the geoid (an equipotential surface) having the same potential as mean sea level at a right angle, and the corresponding point on the surface of the earth [23]. The heights mathematically orthometric height of a point is defined as its geopotential number divided by the mean gravity along the plumbline between that point and the geoid [26]. The geopotential number, defined as the difference between the potential on the geoid and the potential at a surface point. It is determined from the observed gravity and height differences between that point and mean sea level, realized the surface of the Earth [26].

Traditionally height data is obtained from levelling campaigns which results in reduced levels of points. However, the process of levelling is quite laborious, time consuming and expensive usually requiring field observations followed by rigorous post field computations. A minimal cost solution for obtaining orthometric heights is by forecasting using mathematical models. The process of estimating orthometric heights can be problematic due to discrepancies in the estimated values and there is therefore, the necessity of some mathematical modelling to remove discrepancies in the estimated results.

Though there has been extensive work on the application of different techniques in estimating the orthometric of a point [27]. Notable among them are splines and radial basis functions [28], kriging [29], natural neighbour [30,31,32,33,34], rational function models [35], Grobner or Buchberger's algorithm [36] and many more interpolation methodologies [37,38,39,40,41]. Little if any, research has been done on applying plausible alternative technologies such as Polynomial mathematical model, Multivariate Adaptive Regression Splines (MARS), Artificial Neural Networks (ANN) and Multiple Linear Regression (MLR).

[42] used two different polynomial mathematical models, a third degree polynomial regression model and the Thompson's Multiple Variable Polynomial regression models to model the relationship between extracted heights and ground reduced levels. Results from the two models indicates that, the latter presents better refinements to converting extracted heights into reduced levels with a coefficient of determination value of 95.5 %, although further research is recommend to investigate numerical techniques that could improve the solution to the Thompson's polynomial [43]. Many researchers such as [25,44,45,46,47,48] have adopted the polynomial mathematical model to solve some heights problems in mathematical and satellite geodesy.

In the recent decades, artificial neural network (ANN) has been widely adopted and applied to different area of mathematical geodesy. Its suitability as an alternative technique to the classical methods of solving most geodetic problems has been duly investigated [49]. Some of the problems solved in mathematical geodesy include GPS height conversion [50,51,52,53,54], geodetic deformation modelling [55-61], earth orientation parameter determination [62,63,64], precise orbital prediction [65,66], gravity anomaly estimation [67,68,69], geoid determination [70-75], and geodetic coordinate transformation [49,60,76-85]. ANN are been criticized for its long training process in achieving the optimal network's topology, and it is not easy to identify the relative importance of potential input variables, and certain interpretive difficulties [87].

Multivariate Adaptive Regression Splines (MARS) is an adaptive modelling process invented by [88] used for non-linear relationships. In addition, MARS divides the predictor variables into piece-wise linear segments to describe non-linear relationships between the predictor and the dependent variable [87,89]. There are limited availability of literature of MARS in estimating orthometric heights but many studies have successfully applied MARS for solving different problems in engineering. Some of the areas of applications include estimating energy demand [90], slope stability analysis [87,91,92,93], landslide susceptibility mapping [94], water pollution prediction [95], earthquake modelling [96], studying ecological variables [97], region spatio-temporal mapping [98], modelling of the ionosphere [99], geothermal prospect [100] and so on.

Multiple linear regression technique (MLR) was also applied in this study as an alternative mathematical procedure to estimate a local orthometric height. Several studies have been carried out using MLR and simple linear regression (SLR) procedures in coordinate transformation from global to local datum and vice versa [85,101,102,103,104]. It is well acknowledged that, the regression techniques achievable are applicable to surveying and mapping related works [85].

The existing knowledge and publications have not fully addressed the issue of applying alternative techniques in estimating orthometric heights. In addition, upon careful review of existing studies, the authors realized that the utilization of the Polynomial model, ANN, MARS and MLR techniques have not been applied as a practical alternative technology to the existing approaches. This present study for the first time explored the utilization of the polynomial model, ANN, MARS and MLR in estimating orthometric heights. To achieve the aim of this present study, the polynomial model, ANN, MARS and MLR methods were applied.

This study also highlights the comparison between Polynomial model, ANN, MARS and MLR based on the results of statistical performance indicators such as mean (M), mean square error (MSE), root mean square error (RMSE), mean bias error (MBE), mean absolute error (MAE), standard deviation (SD), noise to signal ratio (NSR), correlation of coefficient (R), and correlation of determination ($R^2$). The finding of these statistical indicators models will reveal the working efficiency of the models for orthometric heights estimation. Hence this study will serve as an added contribution to existing knowledge of polynomial model, ANN, MARS and MLR in mathematical geodesy.

In this context, this paper evaluates, compares, and discusses the different methods of estimating the local orthometric height for a local geodetic network. In order to ascertain the efficiency of the methods, the Eastings, Northings and the orthometric heights were applied in the polynomial model, ANN, MARS and MLR models. This study will therefore create the opportunity for geospatial practitioners in Ghana to arrive at a consensus on the most appropriate technique applicable for estimating orthometric heights within the local geodetic datum.

## 2. Study Area and Data Source

The study was carried out in a large scale gold mine, denoted in this study as Mine X. Mine X is situated in the Western part of Ghana (Figure 1), almost 100 km South-West of Kumasi, Ghana's second largest city [105]. The township of the study area lies 15 km North-Northeast of the project area [106]. It covers a land area of 873 $km^2$ and which characterizes 8.6 % of the total land area of the Western Region of Ghana [105]. The land mass is dominated by steep terrain and dense vegetation interspersed with small agricultural plots of palm trees, cassava, and cocoa. The climate is mainly tropical with the highest mean temperature of 34 °C which is recorded between March and April whilst the lowest mean temperature of 30 °C is experienced in August [107]. Mine X lies with the Proterozoic terrain of Southwest Ghana and comprise rocks of Birimian age, with the belt dominated by Mafic volcanic and the basin typical by fine grained, deep water sediment and intruded by granites [106]. The topography of the land is about 350 m to 660 m above mean sea level and it lies beneath the Birimian and Tarkwaian rocks which is rich in minerals such as Bauxite, Manganese, and Gold deposits [108].

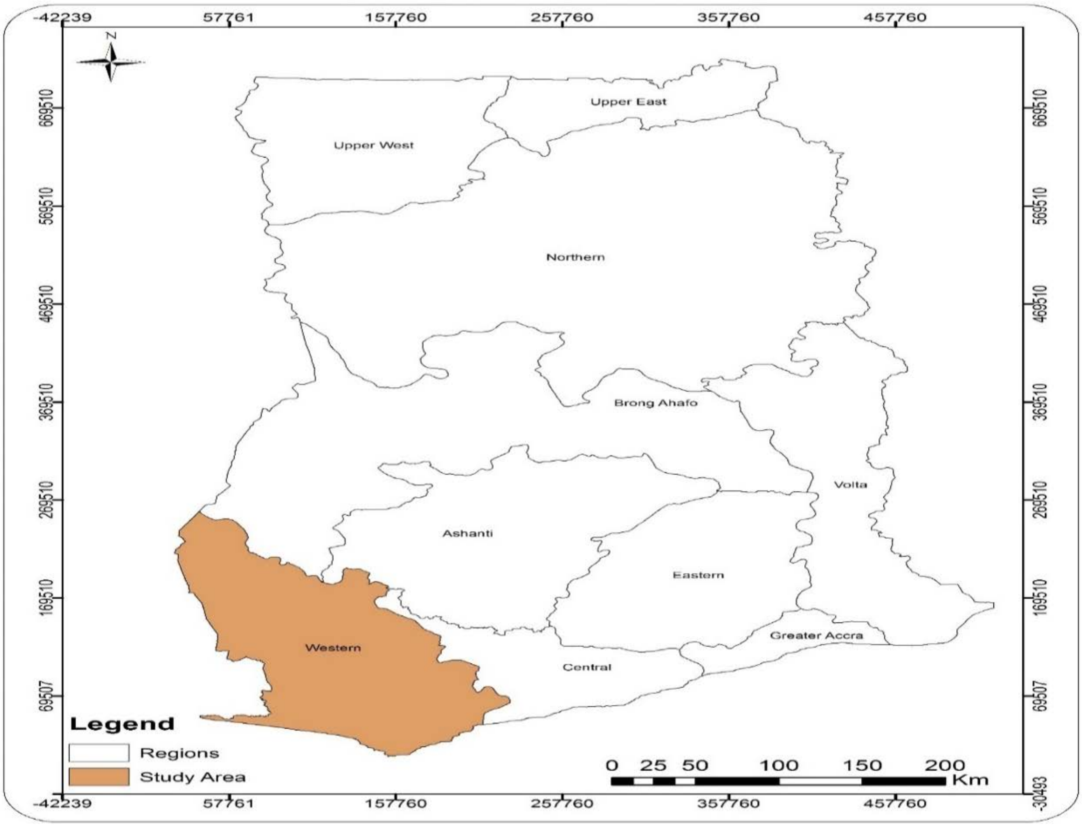


**Figure 1.** The Study Area

**Table 1. Sample of the dataset**

| ID | Y (m) | X (m) | Z (m) |
|---|---|---|---|
| 1 | 116255.701 | 385420.847 | 31.787 |
| 2 | 116280.604 | 385425.436 | 32.064 |
| 3 | 116283.554 | 385402.716 | 32.329 |
| 4 | 116305.495 | 38403.054 | 32.642 |
| 5 | 116305.138 | 385425.242 | 32.314 |
| 6 | 116306.489 | 385453.829 | 32.093 |
| 7 | 116282.872 | 385450.118 | 31.625 |
| 8 | 116258.058 | 385446.191 | 31.538 |
| 9 | 116258.906 | 385466.920 | 31.273 |
| 10 | 116260.631 | 385486.351 | 31.007 |

Dataset and creation of a spatial database of descriptive variables are significant parts of any study [109]. Topographical data from Mine X were obtained from the Mine to embark this present study. The data consists of Easting, Northing, and Elevation of the observed prisms position. The data consists of 2280 field points obtained during a mini project in Mine X. Table 1 shows a sample of the dataset used to embark this present study.

## 3. Methods

### 3.1. Polynomial Mathematical Model

Polynomial mathematical models are used to represent the terrain surfaces in the global, regional, local and patchwise methods of interpolations [110]. The basic general polynomial equation for surface representation is shown by Equation 1 below, where $Z_i$ is the height of an individual point $i$ , $x_i$ and $y_i$ are the rectangular coordinates of the point $i$ and $a_0$, $a_1$, $a_2$ .... $a_{15}$ are the coefficients of the polynomial. One such equation will be generated for each individual point $i$ with coordinates $x_i$ , $y_i$ in estimating the $Z_i$ using the linear bi-saddle polynomial mathematical model given by Equation 1 as:

$$Z_i = a_0 + a_1 x_i + a_2 y_i + a_3 x_i y_i. \tag{1}$$

The coefficients were determined using the ordinary least square and total least square techniques.

### 3.2. Ordinary Least Square (OLS) and Total Least Square (TLS)

Least Square method is a statistical technique that is capable of determining the line of best fit of a model and seeks to find the minimum sum of the squares of residuals. This method is extensively used in regression analysis and estimation [111]. Considering a system of equations in the form as denoted by Equation 2 to be solved by least squares:

$$BX \approx L \tag{2}$$

Where $B \in R^{m\times n}$, $X \in R^{n\times d}$, $L \in R^{m\times d}$ , and $m \geq n$ . Where m is the number of rows and n is the number of columns [112,113].

The solution of the unknown parameters matrix X by OLS approach can be achieved as denoted by Equation 3:

$$X = \left[B^T B\right]^{-1}\left[B^T L\right]. \tag{3}$$

The corresponding error vector V can be achieved by using Equation 4 as denoted by:

$$V = BX - L. \tag{4}$$

On the other hand, solution of unknowns' parameters $\hat{X}$ by TLS approach is obtained as denoted by Equation 5:

$$L + V_L = \left[B + V_B\right]\hat{X} rank(B) = m < n \tag{5}$$

Where $V_L$ is the error vector of observations and $V_B$ is the error matrix of the data matrix, the assumption that both have independently and identically distributed rows with zero mean and equal variance [114].

[115], invented TLS to rectify the inefficiency associated with the OLS. Thus, accounting for perturbations in data matrix and observation matrix [116]. TLS is a mathematical algorithm that yields a unique solution in analytical form in terms of the Singular Value Decomposition (SVD) of the data matrix [117]. According to [115] and [118], the TLS algorithm is an iterative process which looks to minimize the errors in Equation 6 as denoted by:

$$\min \left\| [B, L] - \left[\hat{B}, \hat{L}\right] \right\|_F, \left[\hat{B}, \hat{L}\right] \in R^{n(m+1)}. \tag{6}$$

The optimization process goes on until a minimizing $\left[\hat{B}, \hat{L}\right]$ is obtained, any $\hat{X}$ that satisfies $\hat{B}\hat{X} = \hat{L}$ is the TLS solution [112]. In order to obtain the solution of $B\hat{X} = L$ , we write the functional relation as denoted by Equation 7:

$$[B, L]\left[X^T, -1\right]^T \approx 0. \tag{7}$$

The TLS problem can be solved using the Singular Value Decomposition (SVD) [117,119]. The SVD of the augmented matrix $[B, L]$ is required to determine whether or not it is rank deficient. Matrix $[B, L]$ can be represented by SVD as denoted by Equation 8 as:

$$[B, L] = USV^T \tag{8}$$

Where U = real valued m x n orthonormal matrix, $UU^T$ = Im, V = real value n x n orthonormal matrix, $VV^T$ = In, S = m x n matrix with diagonals being singular values, off-diagonals are zeros. The rank of matrix $[B, L]$ is m + 1, and must be reduced to m using the Eckart-Young Mirsky theorem [116]. The TLS solution after the rank reduction is given by Equation 9 denoted as:

$$\left[\hat{X}^T, -1\right] = \frac{1}{V_{m+1,m+1}} V_{m+1}. \tag{9}$$

If $V_{m+1,m+1} \neq 0$ , then

$$BX = L = -1/(V_{m+1,m+1}).B\left[V_{1,m+1}, \cdots, V_{m,m+1}\right]^T$$

belongs to the column space of $\hat{B}$, hence X solves the basic TLS problem [120]. The corresponding TLS correction is achieved by using Equation 10 as denoted by:

$$\left[\Delta\hat{B}, \Delta\hat{L}\right] = [B, L] - \left[\hat{B} - \hat{L}\right]. \tag{10}$$

## 3.3. Artificial Neural Network (ANN)

### 3.3.1. Normalization

In training dataset with ANN model, the dataset must be normalized. The original data to be used for the ANN training and its model formulation are expressed in different units with different physical meanings. Therefore, to ensure constant variation in the ANN model, datasets are frequently normalized to a certain interval such as [-1, 1], [0, 1] or other scaled criteria. This data normalization improves convergence speed and doing so reduces the chances of getting stuck in local minima. In this study, the selected input and output variables were normalized into the interval [−1, 1] according to Equation 11 denoted as [121]:

$$y_i = y_{\min} + \frac{\left(y_{\max} - y_{\min}\right) \times \left(x_i - x_{\min}\right)}{\left(x_{\max} - x_{\min}\right)} \tag{11}$$

Where $y_i$ represents the normalized data, $x_i$ is the measured coordinate value, while $x_{\min}$ and $x_{\max}$ represent the minimum and maximum values of the measured coordinates with $y_{\max}$ and $y_{\min}$ values set at 1 and -1, respectively.

### 3.3.2. ANN Architecture

In this study, the adopted supervised ANNs architecture namely BPNN was utilized due to its frequent application. The networks have a feed forward topology consisting of input, hidden and output layers that are fully interconnected.

### 3.3.3. Backpropagation Neural Network (BPNN)

The backpropagation neural network (BPNN) has gained much popularity over the last decade and has many application areas in geodesy [60,78,79,82,83,84]. The BPNN encompasses an input layer, one or more hidden layers and an output layer of processing neurons with each layer feeding input to the next layer in a feedforward fashion through a set of connection weights [122]. The input layer is an opening that is responsible for receiving the input data, whereas the output layer gives the final results of the computation. In between these two layers is the hidden layer chamber where the input data are fed to the neurons in the hidden layer for processing. It is important to state that the connections between all the layers of the network are realized through synaptic weights, which are in turn used by the network to solve a specific problem. It is also well acknowledged that the number of hidden neurons, hidden layers and type of activation functions used in the BPNN determines its competency. Typically, the number of hidden neurons is obtained through the sequential trial and-error approach. This is partly due to the type of problem at hand, the choice of neural network architecture and the proposed theoretical concepts that are yet to be universally accepted to clarify the number of hidden neurons needed to approximate a given function. In this study, the optimum number of hidden neurons was obtained based on the lowest mean squared error (MSE). The MSE is represented by Equation (12) as:

$$MSE = \frac{1}{n}\sum_{i=1}^{n}\left(\alpha_i - \beta\right)_i^2 \tag{12}$$

Where $\alpha_i$ and $\beta$ are the measured and predicted plane displacements from the BPNN model. The present study applied one hidden layer in the BPNN. This decision was in line with the conclusion made in [123], that the BPNN with one hidden layer could be used as a universal approximate for any discrete and continuous functions. Furthermore, to introduce non-linearity into the network, the hyperbolic tangent activation function was selected for the hidden units, while a linear function was applied for the output units. The hyperbolic tangent function [124] is defined in Equation (13) denoted as:

$$f(x) = \tanh(x) = \frac{2}{1+e^{-2x}} - 1 \tag{13}$$

Where $x$ is the sum of the weighted inputs. It worth stating that the BPNN training can be considered as a non-linear optimization problem, $w^*$ (Konaté *et al.*, 2015), given by Equation (14) denoted as:

$$w^* = \arg\min E(w) \tag{14}$$

Where $w$ is the weight matrix and $E(w)$ is the error function. The purpose of training the network is to find the optimal weight connection $\left(w^*\right)$ that minimizes $E(w)$ such that the estimated outputs from the BPNN will be in good agreement with the target data. This $E(w)$ is evaluated at any point of $w$ shown in Equation (15) as denoted by:

$$E(w) = \sum_n E_n(w) \tag{15}$$

Where $n$ is the number of training samples and $E_n(w)$ is the output error for each sample $n$. $E_n(w)$ [125,126] is mathematically defined by Equation (16) denoted as:

$$E_n(w) = \frac{1}{2}\sum_j\left(d_{nj} - y_{nj}(w)\right)^2 \tag{16}$$

Where $d_{nj}$ and $y_{nj}(w)$ are anticipated network outputs and estimated values of the $jth$ output neuron for the nth sample, respectively. Therefore, substituting Equation (14) into Equation (17) gives the objective function to be minimized expressed in Equation (17) as given as:

$$E(w) = \frac{1}{2}\sum_n\sum_j\left(d_{nj} - y_{nj}(w)\right)^2. \tag{17}$$

### 3.4. Multivariate Adaptive Regression Splines (MARS

The MARS model uses a nonparametric modelling approach that does not require assumptions about the form of the relationship between the independent and dependent variables [88,109]. The MARS model works by dividing the ranges of the explanatory variables into regions and by producing for each of these regions a linear regression equation [109]. The breaks values between each region are called knots, whiles the term basis functions (BFs) are used to demonstrate each distinct interval of the predictors [96,109]. BFs are functions of the following form as denoted by Equation 18:

$$\max(0, x-k) \ or \ \max(0, k-x) \tag{18}$$

Where x is an independent variable and k is a constant corresponding to a knot [109]. The general formula for the MARS model is given by Equation 19 as denoted by [87]:

$$y = f(x) = a_0 + \sum_{n=1}^{N} \alpha_n \beta_n(x) \tag{19}$$

Where, $y$ is the dependent variable predicted by the function $f(x)$, $a0$ is a constant, and $N$ is the number of terms, each of them formed by a coefficient $\alpha_n$ and $\beta_n(x)$ is an individual basis functions or a product of two or more BFs. The MARS model was developed in two steps. In the first step, the forward algorithm, basis functions are presented to define Equation 19. Many basis functions are added in Equation 19 in order to get a better result [96,109]. The developed MARS may experience over fitting due to the large number of basis functions. In order to mitigate this problem, the second step that is the backward algorithm prevents over fitting by removing redundant basis functions from Equation 19. The MARS model adopts Generalized Cross-Validation (GCV) to delete the redundant basis functions (Samui and Kothari, 2012). The expression of GCV is written as (Craven and Wahba, 1979):

$$GCV = \frac{\frac{1}{N}\sum_{i=1}^{N}\left[y_i - \dot{f}(x_i)\right]^2}{\left[1 - \frac{C(H)}{N}\right]^2} \tag{20}$$

Where $N$ is the number of data and $C(H)$ is a complexity penalty that increases with the number of basis function (BFs) in the model and which is defined as denoted by Equation 21:

$$C(H) = (h+1) + dH \tag{21}$$

Where $d$ is a penalty for each BFs included into the model and $H$ is the number of basis functions in Equation 10 [88,127].

### 3.6. Multiple Linear Regression (MLR)

The multiple linear regression (MLR) is an extensively used techniques in geoscientific studies for articulating the dependence of a response variable on several explanatory variables [85]. It fits a linear combination of the components of multiple input parameters to a single output parameter defined by Equation (22) as:

$$y = \alpha_0 + \sum_{i=1}^{M} \beta_i x_i \tag{22}$$

Where $\alpha_0$ is the intercept (values when all the independent variables are zero) with $\beta_i$ values denoting the regression coefficients which were obtained in this present study using the least square technique. In Equation (22), $i$ is an integer varying from 1 to M, where M is the total number of observations. Since there are several variables that can be used as candidates for predictor variables in the MLR models formulation, it would be demanding having to try every possible combination of variables [85].

### 3.7. Model Performance Assessment

In order to compare the models results with the estimated heights, the residuals calculated between the desired outputs and the outputs produced by the various techniques were utilized. Hence, to make an objective assessment of the models, performance criteria indices (PCI) of mean error (ME), mean square error (MSE), root mean square error (RMSE), mean bias error (MBE), standard deviation (SD), noise to signal ratio (NSR), correlation coefficient (R), correlation of determination ($R^2$) were adopted. Their mathematical representation is given by Equation (23) to Equation (33) as follows:

$$ME = \frac{1}{n}\sum_{i=1}^{n}(\alpha_i - \beta_i) \tag{23}$$

$$MSE = \frac{1}{n}\sum_{i=1}^{n}(\alpha_i - \beta_1)^2 \tag{24}$$

$$RMSE = \sqrt{\sum \frac{E^2}{n}} \tag{25}$$

$$MBE = \sqrt{\sum \frac{E}{n}} \tag{26}$$

$$MAE = \sqrt{\sum \frac{|E|}{n}} \tag{27}$$

$$SD = \sqrt{\frac{1}{n-1}\sum_{i=1}^{n}(e - \bar{e})^2} \tag{28}$$

$$SNR = \frac{Average\ of\ theresiduals}{SD\ of\ theresiduals} \tag{29}$$

With reference to Equations (23) to (27), $n$ is the total number of points, $\alpha_i$ and $\beta_i$ are the measured variable and estimated variable produced by the models. $\alpha$ represent the residuals between the measured and estimated variables and $\bar{\alpha}$ is the mean value of the residuals. $| \ |$ in Equation (27) represents the absolute value of the residuals estimated between $\alpha_i$ and $\beta_i$. $E$ is the average of the residuals. The correlation coefficient (R) is given by Equation (30) as:

$$R=\left(\frac{\sum_{i=1}^{N}(\alpha_i-\bar{\alpha})(\beta_i-\bar{\beta})}{\sqrt{\sum_{i=1}^{N}(\alpha_i-\bar{\alpha})}^2\times\sqrt{\sum_{i=1}^{N}(\beta_i-\bar{\beta})^2}}\right) \quad (30)$$

Where $N$ is the total number of test examples presented to the learning algorithms, $\alpha$ and $\beta$ are the measured and predicted plane coordinates from the various procedures, while $\bar{\alpha}$ and $\bar{\beta}$ are the mean of the predicted ionospheric delay corrections. $e$ in Equation (28) denotes the residual between the measured and predicted ionospheric delay corrections, and $\bar{e}$ is the average of the residual. The $R^2$ was computed by Equation (31) as:

$$R^2=\left(\frac{\sum_{i=1}^{N}(\alpha_i-\bar{\alpha})(\beta_i-\bar{\beta}_i)}{\sqrt{\sum_{i=1}^{N}(\alpha_i-\bar{\alpha})}\times\sqrt{\sum_{i=1}^{N}(\beta_i-\bar{\beta}_i)^2}}\right)^2 \quad (31)$$

Where $R^2$ is the correction of determination and the other variables are the same as in defined in Equation 30. $N$ is the total number of test examples presented to the learning algorithms, $\alpha$ and $\beta$ are the measured and predicted plane coordinates from the various procedures, while $\bar{\alpha}$ and $\bar{\beta}$ are the mean of the predicted ionospheric delay corrections.

## 4. Results and Discussions

The undetermined parameters of simple planar surface polynomial model were achieved by utilizing the OLS and TLS models. The unknown parameters with their individual standard deviation are tabulated in Table 2 below. Sample of the results achieved by the OLS and TLS using the polynomial is tabulated in Table 3. Figure 2 represent the 3D surface map and contour generated from the observed data. Figure 3 is the results of the 3D surface map and contour map generated from the OLS model using the polynomial approach, and Figure 4 is the results of the 3D surface map and contour map obtained from the TLS model using the polynomial approach. The performance criteria indices of the OLS and TLS models using the polynomial technique are tabulated in Table 3 below.

**Table 2. Parameters obtained by the OLS and TLS models (Units in metres)**

| OLS | | | TLS | | |
|---|---|---|---|---|---|
| VALUE | PARAMETER | SD | VALUE | PARAMETER | SD |
| a0 | 845.1159 | 34.3072000 | a0 | 1.0354E04 | 1.1232E-05 |
| a1 | -0.00270 | 7.6967E-05 | a1 | -0.0239000 | 2.5198E-11 |
| a2 | 0.002000 | 5.0263E-05 | a2 | -0.0096000 | 1.6456E-11 |

**Table 3. Sample results by the OLS and TLS models (Units in metres)**

| OLS | | | TLS | | |
|---|---|---|---|---|---|
| ACTUAL | PREDICTED | RESIDUAL | ACTUAL | PREDICTED | RESIDUAL |
| 31.787 | 36.9910151 | -5.20402 | 31.787 | 26.3870271 | 5.399973 |
| 32.064 | 37.0284308 | -4.96443 | 32.064 | 26.0382812 | 6.025719 |
| 32.329 | 37.095678 | -4.76667 | 32.329 | 26.5529692 | 5.776031 |
| 32.642 | 37.1386442 | -4.49664 | 32.642 | 26.3342574 | 6.307743 |
| 32.314 | 37.0780886 | -4.76402 | 32.314 | 25.8073914 | 6.506609 |
| 32.093 | 37.0035397 | -4.91054 | 32.093 | 25.1111925 | 6.981808 |
| 31.625 | 36.9663254 | -5.34133 | 31.625 | 25.4266086 | 6.198391 |
| 31.538 | 36.9273003 | -5.3893 | 31.538 | 25.7586783 | 5.779322 |
| 31.273 | 36.873028 | -5.60003 | 31.273 | 25.2551144 | 6.017886 |
| 31.007 | 36.8240143 | -5.81701 | 31.007 | 24.7741535 | 6.232847 |

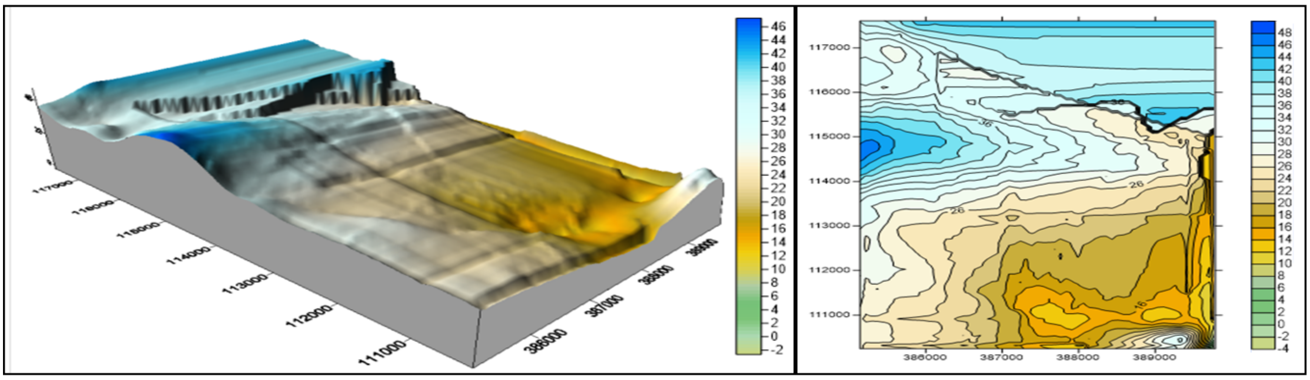

**Figure 2**. 3D and Contour map of the observed data

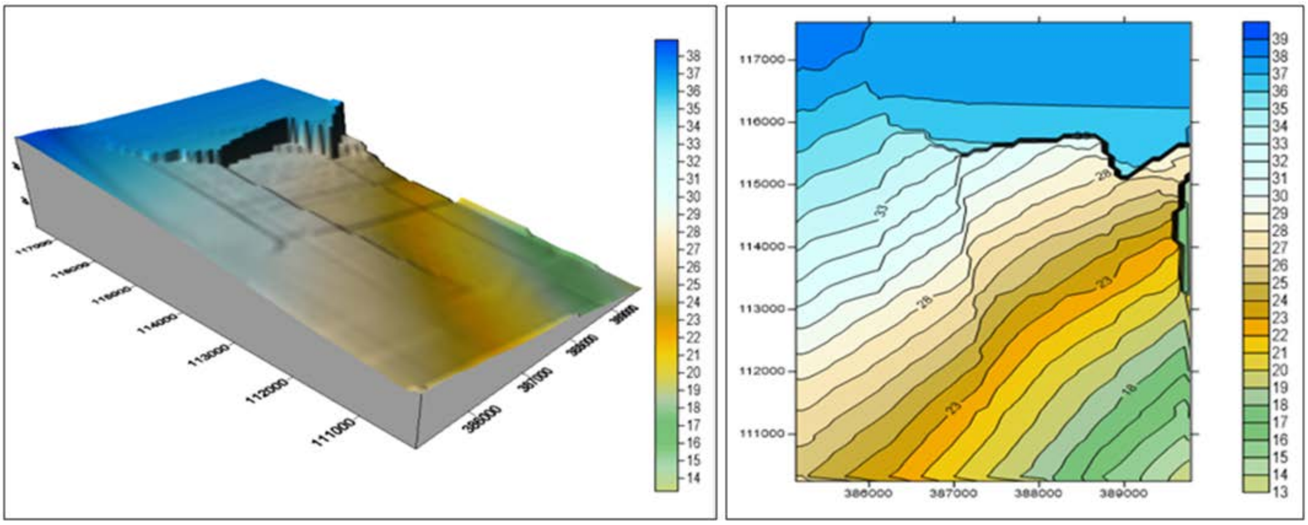


**Figure 3.** 3D and Contour map results by the OLS model

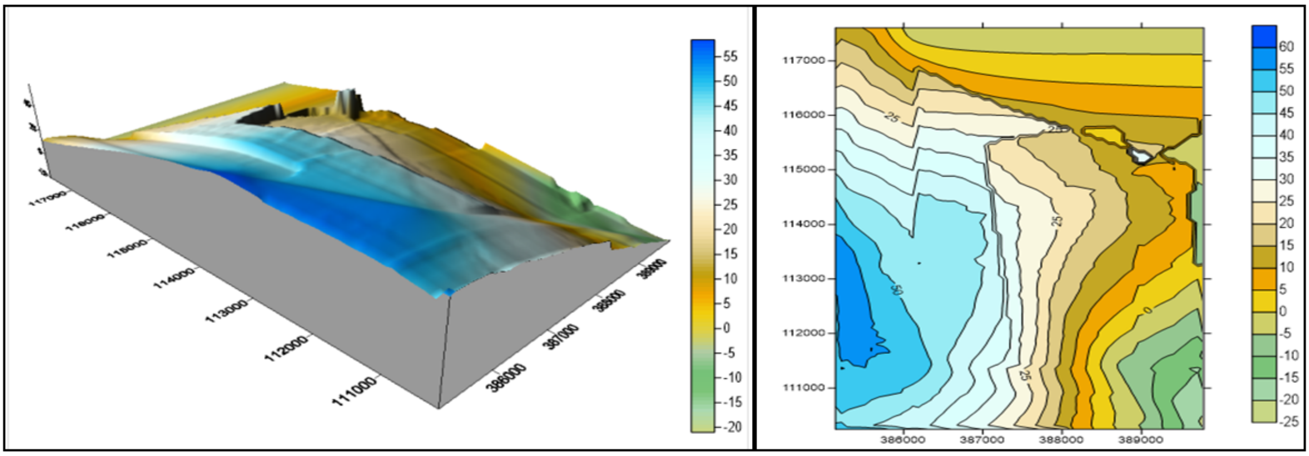


**Figure 4.** 3D and Contour map results by the TLS model

**Table 4. Statistical analysis of the OLS and TLS models (Units in metres)**

| PCI | M | MSE | RMSE | MAE | MBE | SD | NSR |
|---|---|---|---|---|---|---|---|
| OLS | -0.13571 | 38.20282 | 6.180843 | 0.368388 | 0.368388 | 38.1844 | 0.00355 |
| TLS | 0.683455 | 68.3294 | 21.64092 | 0.826714 | 0.826714 | 0.009206 | 74.23796 |

**Table 5. Sample results by the MARS and MLR models (Units in metres)**

| MARS | | | MLR | | |
|---|---|---|---|---|---|
| ACTUAL | PREDICTED | RESIDUAL | ACTUAL | PREDICTED | RESIDUAL |
| 31.787 | 31.9548 | -0.1678 | 31.787 | 38.0300413 | -6.24304 |
| 32.064 | 31.8838 | 0.1802 | 32.064 | 38.1132174 | -6.04922 |
| 32.329 | 32.1478 | 0.1812 | 32.329 | 38.1230704 | -5.79407 |
| 32.642 | 32.1286 | 0.5134 | 32.642 | 38.1963533 | -5.55435 |
| 32.314 | 31.8691 | 0.4449 | 32.314 | 38.1951609 | -5.88116 |
| 32.093 | 31.5334 | 0.5596 | 32.093 | 38.1996733 | -6.10667 |
| 31.625 | 31.5932 | 0.0318 | 31.625 | 38.1207925 | -6.49579 |
| 31.538 | 31.6564 | -0.1184 | 31.538 | 38.0379137 | -6.49991 |
| 31.273 | 31.4131 | -0.1401 | 31.273 | 38.040746 | -6.76775 |
| 31.007 | 31.1844 | -0.1774 | 31.007 | 38.0465075 | -7.03951 |

From Table 2 above, it was observed that both OLS and TLS using the polynomial approach produce satisfactory results of the orthometric heights in the mine but with less accuracies. From Figure 2, Figure 3, and Figure 4, it can be observed that both models are not fitting the actual terrain in the mine. This means that, in this present study, both the OLS and TLS using the simple planar surface is inefficient in estimating orthometric heights in the mine. This can be attribute to the inability of both models to denoise the dataset to give a better estimate of the orthometric heights. In this present study, the OLS approach as compare to the TLS achieve higher results in terms of accuracy in estimating the orthometric heights using the polynomial model approach.

Sample of results achieved by the MARS and MLR models are tabulated in Table 5. 25 basis functions have been used to construct the MARS model. 3D and contours maps generated by the MARS and MLR models results is represented by Figure 5 and Figure 6 below. Their performance criteria indices is tabulated in Table 6 below. Ultimately, 14 basis functions have been used for the optimum MARS model. The final equation for prediction of the orthometric height in the mine using the MARS model is given by Equation 32:

$$y(i) = -8.050763 + \sum_{n=1}^{14} \alpha_i \beta_i \tag{32}$$

The optimal equation developed by the MLR model for estimating orthometric heights in the mine is denoted by Equation 33 as given by:

$$y(i) = -350.264 + (0.00334 * Y(i)) \tag{33}$$

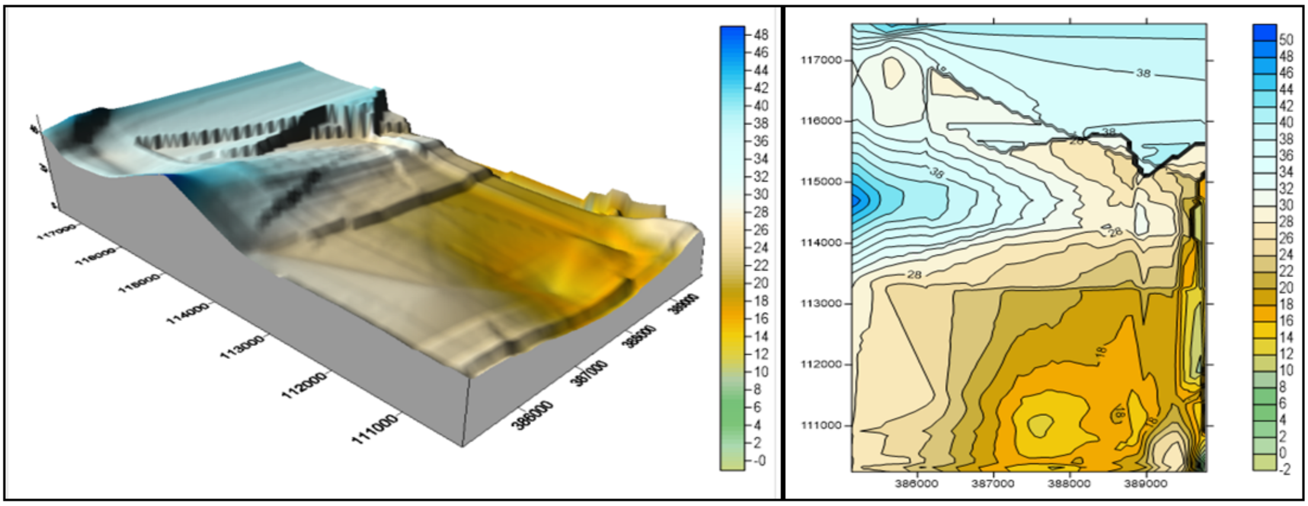

**Figure 5.** 3D and Contour map by the MARS model

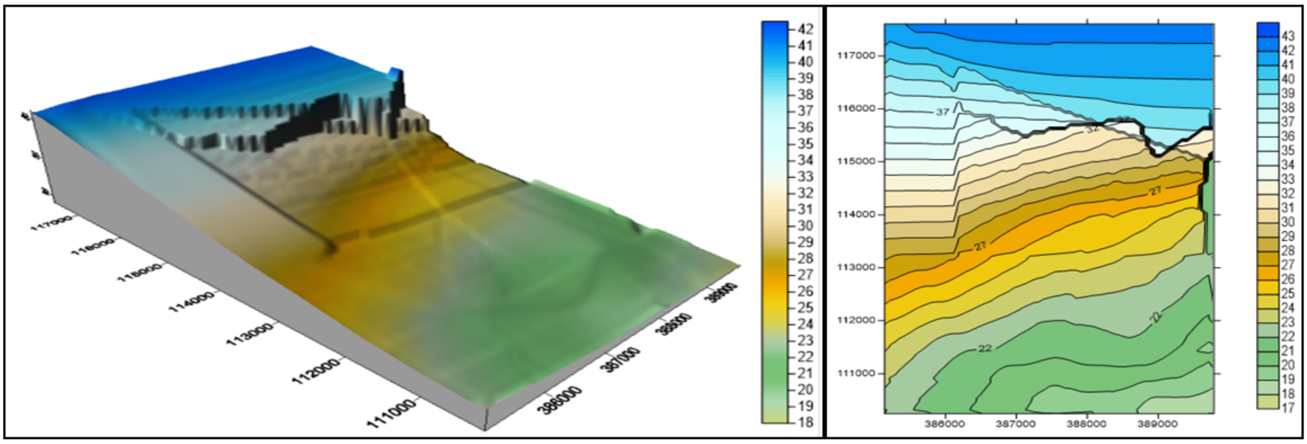

**Figure 6.** 3D and Contour map by the MLR model

**Table 6. Statistical analysis of the MARS and MLR model (Units in metres)**

| PCI | M | MSE | RMSE | MBE | MAE | SD | NSR |
|---|---|---|---|---|---|---|---|
| MARS | -1.89E-6 | 2.246374 | 1.498791 | 0.001374 | 0.001374 | 2.24736 | 8.40E-7 |
| MLR | -0.36657 | 45.1855 | 6.722016 | 0.60545 | 0.60545 | 0.60545 | 47.9877 |

The statistical findings reveals that the MARS models produce satisfactory results with higher accuracy in estimating orthometric heights in the mine. MARS compare to the MLR and polynomial model can be used as a plausible alternative technique in estimating orthometric heights in the mine.

**Table 7. ANN optimal results**

| PCI | MSE | R |
|---|---|---|
| TRAINING | 9.28E-02 | 9.99E-01 |
| VALIDATION | 1.07E-01 | 9.99E-01 |
| TESTING | 9.38E-02 | 9.9E-01 |

**Table 8. Sample results by the ANN model (Units in metres)**

| ACTUAL | PREDICTED | RESIDUAL |
|---|---|---|
| 17.169 | 16.9433723 | 0.225628 |
| 28.381 | 28.8483558 | -0.46736 |
| 18.486 | 18.6306682 | -0.14467 |
| 18.354 | 18.3718239 | -0.01782 |
| 20.677 | 20.3382698 | 0.33873 |
| 20.387 | 20.3777289 | 0.009271 |
| 20.696 | 20.6816927 | 0.014307 |
| 22.454 | 22.3169044 | 0.137096 |
| 22.52 | 22.3092293 | 0.137096 |
| 23.123 | 22.5970152 | 0.525985 |

**Table 9. Statistical analysis of the ANN model (Units in metres)**

| PCI | M | MSE | RMSE | MAE | MBE | SD | NSR |
|---|---|---|---|---|---|---|---|
| ANN | 0.005835 | 0.095055 | 0.30831 | 0.076385 | 0.076385 | 0.095063 | 0.061378 |

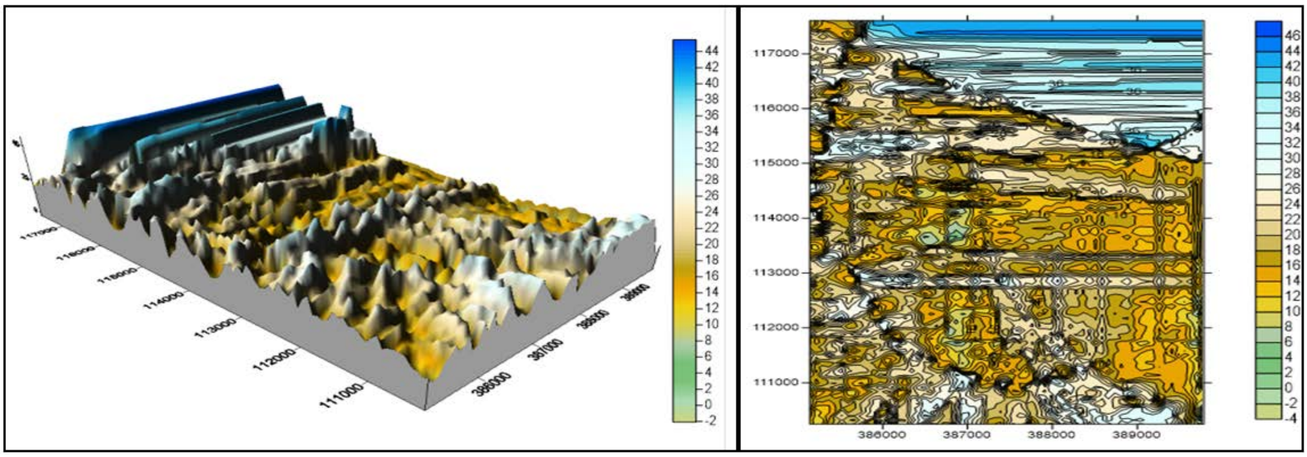


**Figure 7**. 3D and Contour map by the ANN model

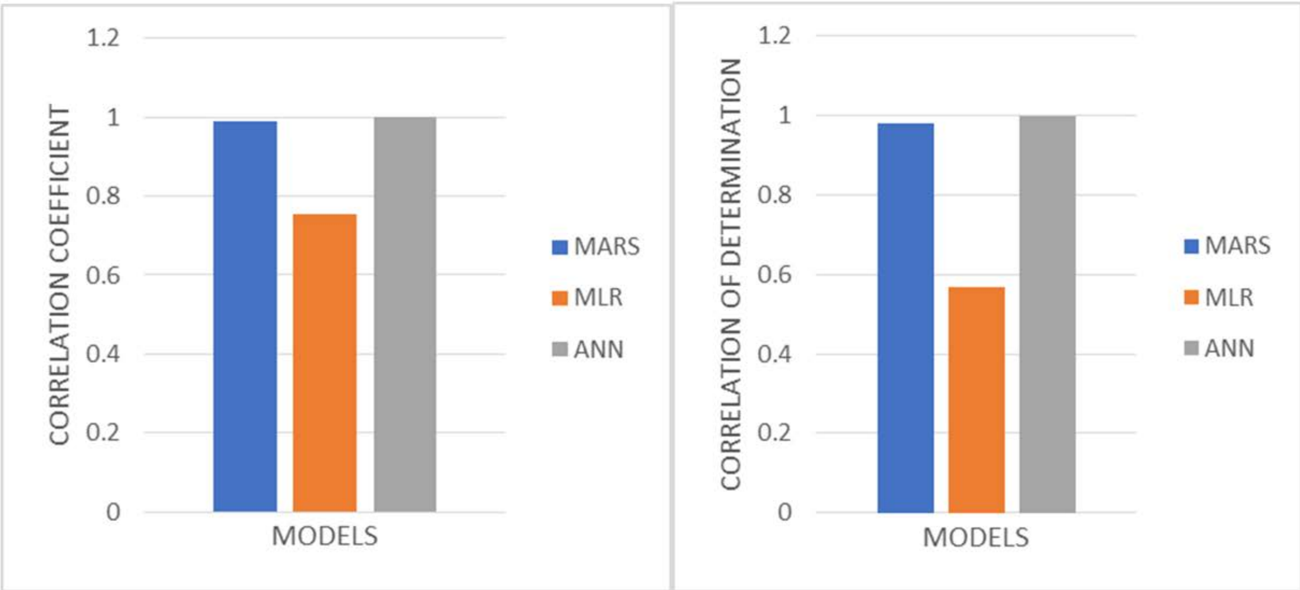


**Figure 8**. Correlation results

The optimal ANN model achieved in this present study was 2-18-1, thus 2 inputs, 18 hidden neurons and 1 output. The model was trained with 25 hidden neurons. The 18 hidden neuron was the optimal ANN structure that achieved a lesser MSE and higher R value. The results for the optimal ANN structure is tabulated in Table below. Sample of the results obtained by the ANN model is tabulated in Table 8 with their performance criteria indices and 3D and contour map represented by Table 9 and Figure 7. According to their statistical finings, the ANN as compare to the MARS model produce satisfactory results in the estimating of orthometric heights in the mine with good results in terms of accuracy.

The correlation coefficient and correlation of determination results which shows the relationship between the input values (independent variables) and output (dependent variables) is represent by Figure 8. It can be observed there is a higher correlation relationship between the ANN and MARS models in estimating the orthometric heights in the mine.

## 5. Concluding Remarks

In this present study, we proposed various methods for estimating orthometric heights in a mine based on the utilization of the polynomial, ANN, MARS and MLR models. Through the analysis of the statistical findings of each model, the results shows that, the proposed ANN and MARS model is feasible for estimating orthometric heights in the mine. In addition, we draw conclusions from the results achieved in this present study that, the MARS and ANN models can be used as a plausible alternative techniques in estimating orthometric heights for an area of interest. This study will create the opportunity for geospatial practitioners to know the efficiency of polynomial, ANN, MARS and MLR in solving some of the problems in geoscientific communities.

# Acknowledgements

The authors wish to acknowledge the assistance given by many reviewers and individuals. They have supplied a great deal of relevant and interesting material, much of which has had to be condensed considerably to fit within the scope of this paper. Nevertheless, sincere thanks are due to all of those whose have contributed information used in this paper.

# References

[1] Heiskanen, W. A., and Moritz, H., "*Physical Geodesy*", San Francisco, WH Freeman, 1967.

[2] Vanicek, P., and Krakiwsky, E., "*Geodesy the Concepts*", 2nd edn., Elsevier, Amsterdam, 1986.

[3] Tenzer, R., and Vanicek, P., and Santos, M., "Mean gravity along the plumbline", *In: Paper presented to the CGU and AGU annual scientific meeting*, Montreal, 2004.

[4] Strang van Hees, G. L., "Practical formulas for the computation of the Orthometric and dynamic correction", *Zeitschrift fur Vermessungswesen*, 1992, 117.

[5] Drewes, H., Dodson, A. H., Fortes, L. P., Sanchez, L., and Sandoval, P., "Vertical referencing systems", *IAG Symposia 24, Springer*, Berlin Heidelberg New York, 2002, 353.

[6] Lilje, M., "*Geodesy and Surveying in the future – the importance of heights*", LMV Rep. 1999.3, National Land Survey, Gavle, Sweden, 1999, 418.

[7] Helmert, F. R., "*Die Schwerkraft im Hochgebirge, insbesondere in den Tyroler Alpen*", Veroff. Konigl. Preuss. Geod. Inst., 1890, 1.

[8] Niethammer, T., "*Nivellement und Schwere als Mittel zur Berechnung wahrer Meereshohen*", Schweizerische Geodatische Kommission, 1932.

[9] Mader, K., "Die orthometrische Schwerekorrektion des Prazisions-Nivellements in den Hohen Tauern", *Osterreichische Zeitschrift fur Vermessungswesen*, Sonderheft 15, 1954.

[10] Vanicek, P., Huang, J., Novak, P., Pagiatakis, S. D., Veronneau, M., Martinec, Z., and Featherstone, W. E., "Determination of the boundary values for the Stokes-Helmert problem", *J. Geod*, 73, 180-192, 1999.

[11] Allister, N. A., and Featherstone, W. E., "Estimation of Helmert Orthometric heights using digital barcode levelling, observed gravity and topographic mass-density data over part of Darling Scarp, Western Australia", *Geom Res Aust*, 75, 25-52, 2001.

[12] Hwang, C., and Hsiao, Y. S., "Orthometric height corrections from levelling, gravity, density and elevation data: A Case Study in Taiwan", *J. Geod*, 77(5-6), 292-302, 2003.

[13] Ledersteger, K., "Der Schwereverlauf in den Lotlinien und die Berechnung der wahren Geoidschwere", *Publication dedicated to W. A. Heiskanen, Publ. Finn. Geod Inst*., 46, 109-124, 1955.

[14] Rapp, R. H., "The Orthometric height", *MS Thesis*, Department of Geodesi Science, Ohio State University, Columbus, 1961.

[15] Krakiwsky, E. J., "Heights", *MS Thesis*, Department of Geodesic Science and Survey, Ohio State University Columbus, 1965, 157.

[16] Strange, W. E., "An evaluation of Orthometric height accuracy using borehole gravimetry", *Bull Geod*, 8, 300-311, 1982.

[17] Sunkel, H. , "Digital height and density model and its use for the Orthometric height and gravity field determination for Australia", *In: Proceedings of International Symposium on the definition of the geoid*, Florence, 1986, 599-604.

[18] Kao, S. P., Rongshin, H., and Ning, F. S., "Results of field test for computing Orthometric correction based on measured gravity", *Geom Res Aus*, 72, 43-60, 2000.

[19] Tenzer, R., and Vanicek, P., "Correction to Helmert's Orthometric height due to actual lateral variation of topographical density", *Brazilian J. Cartography-Revista Brasileira de Cartografia*, 55(2), 44-47, 2003.

[20] Tenzer, R., Vanicek, P., Santos, M., Featherstone, W. E., and Kuhn, M., "The rigorous determination of Orthometric heights", *J. Geod*, 1-11, 2005.

[21] Dennis, M. L., and Featherstone, W. E., "Evaluation of Orthometric and related height systems using a simulated mountain gravity field", *In: Tziavos IN (ed) Gravity and geoid 2002*, Department of Survey and Geodesy, Aristole Univ Thessaloniki, 2003, 389-394.

[22] Octavian Roma, R., "Ways of Determining the Orthometric Heights Using GPS Technology, *FIG Working Week 2004*, Athens, Greece, May 22-27, 2004, 1-10.

[23] Torge, W., "*Physical Geodesy*", 3rd Edition, Walter de Gruyter, Berlin, New York, 2001, 416.

[24] Featherstone, W and Vanicek, P., "*The Role of Coordinate Systems, Coordinates and Heights in Horizontal Datum Transformations*", Western Australian Divisions of Institution of Surveyors and Mapping Sciences, Institute and University of New South Wales, 1998.

[25] Peprah, S. M., Yevenyo, Y. Y., and Issaka, I., "Performance Evaluation of the Earth Gravitational Model (EGM2008) – A Case Study", *South African Journal of Geomatics*, 6(1), (in press), 2017.

[26] Kingdon, R., Vanicek, P., Santos, M., Ellmann, A., and Tenzer, R., "Toward an Improved Orthometric Height System for Canada", *Geomatica*, 59(3), 241-249, 2005.

[27] Erdogan, S., "A Comparison of interpolation methods for producing digital elevation models at the field scale", *In Earth Surface Processes and Landforms*, 34, 366-376, 2009.

[28] Godone, D., and Garnero, G., "The role of morphometric parameters in Digital Terrain Models interpolation accuracy", *European Journal of Remote Sensing*, 46, 198-214, 2013.

[29] Englund, E., and Sparks, A., "Geo-EAS (Geostatistical Environment Assessment Software)", Las Vegas, NY, U.S, *Environmental Protection Agency*, 1988, EPA/600/4.88/033a.

[30] Bater, C. W., and Coops, N. C., "Evaluating error associated with lidar-derived DEM interpolation", *Computers & Geosciences*, 35, 289-300, 2009.

[31] Gold, C. M., "*Surface Interpolation, Spatial adjacency and GIS*", (J. Raper, Ed), Taylor & Francis, 1989.

[32] Sambridge, M., Braun, J., and McQueen, H., "Geophysical parameterization and interpolation of irregular data using natural neighbours", *Geophysical Journal International*, 122, 837-857, 1995.

[33] Watson, D. F., and Philip, G., "Neighbourhood-Based Interpolation", *Geobyte*, 2(2), 12-16, 1987.

[34] Sibson, R., "*A brief description of natural neigbour interpolation*", In V Barnett, editor, Interpreting Multivariate Data, 21-36, Wiley, New York, USA, 1981.

[35] Xianyong, L., and Xiuxiao, Y., "Improvement of the Stability Solving rational polynomial coefficients", *International Archives of the Photogrammetry, Remote Sensing and Spatial Information Science*, 2008, XXXVII.

[36] Martin, B., Klas, J., and Kalle, A., "Fast and Stable Polynomial Equation Solving and its application to computer vision", *International Journal of Computer Vision*, 84(3), 237-256, 2009.

[37] Childs, C., "*Interpolation surfaces in ArcGIS Spatial analyst*", ESRI Education Services, 2004.

[38] Tomlison, R., "Thinking about GIS", *In Geographic Information System Planning for Managers*, 2007, 224.

[39] Fisher, P. F., and Tate, N. J., "Causes and Consequences of error in digital elevation models", *Progress in Physical Geography*, 30(4), 467-489, 2006.

[40] Collins, F. C., "*A Comparison of Spatial Interpolation Techniques in Temperature Estimation*", Blacksburg, VA, Virginia Polytechnic Institute and State University, 1995.

[41] Johnston, K., Ver Hoef, J. M., Krivoruchko, K., and Lucas, N., "*ArcGIS9, using ArcGIS Geostatistical Analysis*", Environmental Research Institute, 2003.

[42] Ayer, J., Agyemang, A. B., Yeboah, F., Osei Jnr, E. M., Abebrese, S., Suleman, I., "A Comparative Analysis of Extracted Heights from Topographic Maps and Measured Reduced Levels in Kumasi, Ghana", *South African Journal of Geomatics*, 5(1), 313-324, 2016.

[43] Thompson, E. H., "Corrections to X-Parallaxes", *The Photogrammetric Records*, 6(32), 202-210, 1968.

[44] Soycan, M., "Determination of Geoid Heights by GPS and Precise Trigonometric levelling, *Survey Review*, 38(299), 387-396, 2014.

[45] Erol B., "An automated height transformation using precise geoid models", *Journal of Scientific Research and Essays*, 6(6), 1351-1363, 2011.

[46] Dawod, G. M., Mohammed, H. F., Ismail, S.S., "Evaluation and adaptation of the EGM2008 geopotential model along the Northern Nile Valley, Egypt: Case Study", *Journal of Surveying*, 136, 36-40, 2010a.

[47] Dawod, G., “Towards the redefinition of the Egyptian geoid: performance analysis of recent global geoid models and digital terrain models”, *Journal of Spatial Science*, 53(1), 31-42, 2008.

[48] Al-Krargy, E. M., Doma, M. I. and Dawod, G. M., “Towards an Accurate Definition of the Local Geoid Model in Egypt using GPS/levelling Data: A Case Study of Rosetta Zone”, *International Journal of Innovative Science and Modern Engineering*, 2(11), 1-6, 2014.

[49] Ziggah, Y. Y., Youjian, H., Tierra, A., Konate, A. A., and Hui, Z., “Performance Evaluation of Artificial Neural Networks for Planimetric Coordinate Transformation-A Case Study, Ghana”, *Arab J Geosci*, 9, 698-714, 2016a.

[50] Fu, B., and Liu, X., “Application of artificial neural network in GPS height transformation”, *Appl Mech Mater*, 501(504), 2162-2165, 2014.

[51] Liu, S., and Li, J., and Wang, S., “A hybrid GPS height conversion approach considering of neural network and topographic correction”, *International Conference on Computer Science and Network Technology*, China, 2011.

[52] Lei, W., and Qi, X., “The application of BP neural network in GPS elevation fitting”, *International Conference on Intelligent Computation Technology and Automation*, Changsha-China, 2010.

[53] Tieding, L., Shijian, Z., and Xijiang, C., “A number of issues about converting GPS height by BP neural network”, *International Conference on Biomedical Engineering and Computer Science (ICBECS)*, Wuhan-China, 2010.

[54] Wu, L. C., Tang, X., and Zhang, S., “The application of genetic neural network in the GPS height transformation”, *IEEE Fourth International Conference on Computational and Information Sciences*, Chongqing-China, 2010.

[55] Bao, H., Zhao, D., Fu, Z., Zhu, J., and Gao, Z. (2011), “Application of genetic algorithm improved BP neural network in automated deformation monitoring”, *Seventh International Conference on Natural Computation*, Shanghai-China, IEEE, 2011.

[56] Du, S., Zhang, J., Deng, Z., and Li, J., “A new approach of geological disasters forecasting using meteorological factors based on genetic algorithm optimized BP neural network”, *Elektronika IR Elektro Technika*, 20(4), 57-62, 2014a.

[57] Du, S., Zhang, J., Deng, Z., and Li, J. “A neural network based intelligent method for mine slope surface deformation prediction considering the meteorological factors”, *TELKOMNIKA Indonesian J Elect Eng*, 12(4), 2882-2889, 2014b.

[58] Gao, C. Y., Cui, X. M., and Hong, X. Q., “Study on the applications of neural networks for processing deformation monitoring data”, *Appl Mech and Mater*, 501(504), 2149-2153, 2014.

[59] Pantazis, G., and Eleni-Georgia, A., “The use of artificial neural networks in predicting vertical displacements of structures”, *Int J Appl Sci Technol*, 3(5), 1-7, 2013.

[60] Yilmaz, I., and Gullu, M, “Georeferencing of historical maps using backpropagation artificial neural network”, *Exp Tech*, 36, 15-19, 2012.

[61] Yilmaz, M., “Artificial neural networks pruning approach for geodetic velocity field determination”, *Bol Cienc Geod*, 19(4), 558-573, 2013.

[62] Liao, D. C., Wang, Q. J., Zhou, Y. H., Liao, X. H., and Huang, C. L., “Long-term prediction of the earth orientation parameters by the artificial neural network technique”, *J Geodyn*, 62, 87-92, 2012.

[63] Schuh, H., Ulrich, M., Egger, D., Muller, J., and Schwegmann, W., “Prediction of earth orientation parameters by artificial neural networks”, *J Geod*, 76, 247-258, 2002.

[64] Yu, L., Danning, Z., and Cai, H., “Prediction of length of day using extreme learning machine”, *Geod Geodyn*, 6(2), 151-159, 2015.

[65] He-Sheng, W., “Precise GPS orbit determination and prediction using $H_\infty$ neural network”, *J Chinese Inst Eng*, 29(2), 11-219, 2006.

[66] Li, X., Zhou, J., and Guo, R., “High-precision orbit prediction and error control techniques for COMPASS navigation satellite”, *Chinese Sci Bull*, 59(23), 2841-2849, 2014.

[67] Hajian, A., Ardestani, E. V., and Lucas, C., “Depth estimation of gravity anomalies using Hopfield neural networks”, *J. Earth Sp Phys*, 37(2), 1-9, 2011.

[68] Hamid, R. S., and Mohammad, R. S., “Neural network and least squares method (ANN-LS) for depth estimation of subsurface cavities case studies: Gardaneh Rokh Tunnel, Iran”, *J. Appl Sci Agric*, 8(3), 164-171, 2013.

[69] Tierra, A. R., and De Freitas, S. R. C., “Artificial neural network: a powerful tool for predicting gravity anomaly from sparse data, Gravity, geoid and space missions”, *International Association of Geodesy Symposia*, Springer, Berlin Heidelberg DA, 2005.

[70] Kavzoglu, T., and Saka, M. H., “Modelling local GPS/Levelling geoid undulations using artificial neural networks”, *J. Geodesy*, 78, 520-527, 2005.

[71] Pikridas, C., Fotiou, A, Katsougiannopoulos, S., and Rossikopoulos, D., “Estimation and evaluation of GPS geoid heights using an artificial neural network model”, *Appl Geomat*, 3, 183-187, 2011.

[72] Stopar, B., Ambrozic T., Kuhar, M., and Turk, G., “GPS-derived geoid using artificial neural network and least squares collocation”, *Surv Rev*, 38(300), 513-524, 2006.

[73] Sorkhabi, O. M., “Geoid determination based on log sigmoid function of artificial neural networks: (a case study: Iran), *J Artif Intell Electr Eng*, 3(12), 18-24, 2015.

[74] Veronez, M. R., Thum, B. A., and De Souza, G. C., “A new method for obtaining geoidal undulations through artificial neural networks”, *7th International Symposium on Spatial Accuracy Assessment in Natural Resources and Environmental Sciences*, 2006, 306-316.

[75] Veronez, M. R., De Souza, G. C., Matsuoka, T. M., Reinhart, A., and Da Silva, R. M. (2011), “Regional mapping of the geoid using GNSS (GPS) measurements and n artificial neural network”, *Remote Sens*, 3, 668-613, 2011.

[76] Gullu, M., “Coordinate transformation by radial basis function neural network”, *Sci Res Essays*, 5(20), 3141-3146, 2010.

[77] Gullu, M., Yilmaz, M., Yilmaz, I., and Turgut, B., “Datum transformation by artificial neural networks for geographic information systems applications”, *International Symposium on Environmental Protection and Planning: Geographic Information Systems (GIS) and Remote Sensing (RS) Applications (ISEPP)*, Izmir-Turkey, 2011, pp. 13-19.

[78] Lin, L. S., and Wang, Y. J., “A study on cadastral coordinate transformation using artificial neural network”, *Proceedings of the 27th Asian Conference on Remote Sensing*, Ulaanbaatar, Mongolia, 2006.

[79] Mihalache, R. M., “Coordinate transformation for integrating map information in the new geocentric European system using artificial neural networks”, *GeoCAD*, 2012, 1-9.

[80] Tierra, A., Dalazoana, R., and De Freitas, S., “Using an artificial neural network to improve the transformation of coordinates between classical geodetic reference frames”, *Comput Geosci*, 34, 181-189, 2008.

[81] Tierra, A. R., De Freitas, S. R. C., and Guevara, P. M. (2009), “Using an artificial neural network to transformation of coordinates from PSAD56 to SIRGAS95”, *Geodetic reference frames, international association of geodesy symposia, Springe,r* 134, 173-178, 2009.

[82] Tierra, A., and Romero, R., “Planes coordinates transformation between PSAD56 to SIRGAS using a multilayer artificial neural network”, *Geod Cartogr*, 63(2), 199-209, 2014.

[83] Turgut, B., “A back-propagation artificial neural network approach for three-dimensional coordinate transformation”, *Sci Res Essays*, 5(21), 3330-3335, 2010.

[84] Zaletnyik, P., “Coordinate transformation with neural networks and with polynomials in Hungary”, *International Symposium on Modern Technologies, Education and Professional Practice in Geodesy and Related Fields*, Sofia, Bulgaria, 2004, 471-479.

[85] Ziggah, Y. Y., Youjian, H., Yu, X., & Basommi, L. P., “Capability of Artificial Neural Network for forward Conversion of Geodetic Coordinates ($\Phi$, $\lambda$, h) to Cartesian Coordinates (X, Y, Z)”, *Math Geosci*, 48, 687-721, 2016b.

[86] Lee, T. S., and Chen, I. F., “A two-stage hybrid credit scoring model using artificial neural networks and multivariate adaptive regression splines”, *Expert Syst Appl*, 28, 743-752, 2005.

[87] Samui, P., “Multivariate Adaptive Regression Spline (MARS) for prediction of Elastic Modulus of jointed Rock Mass”, *Geotech Geol Eng*, 31, 249-253, 2013.

[88] Friedman, J. H., “Multivariate adaptive regression splines”, *Annals Statistics*, 19, 1-67, 199.

[89] Leathwick, J. R, Rowe, D., Richardson, J., Elith, J., and Hastie, T., “Using multivariate adaptive regression splines to predict the distributions of New Zealand’s freshwater diadromous fish”, *Freshw Biol*, 50, 2034-2051, 2005.

[90] Alreja, J., Parab, S., Mathur, S., and Samui, P., "Estimating hysteretic energy demand in steel moment resisting frames using Multivariate Adaptive regression Spline and Least Square Support Vector Machine", *Ains Shams Engineering Journal*, 2015.

[91] Lall, U., Sangoyomi, T., Abarbanel, H. D. I., "Nonlinear dynamics of the Great Salt Lake: nonparametric short term forecasting", *Water Resour Res*, 32, 975-985, 1996.

[92] Attoh-Okine, N. O., Mensah, S., Nawaiseh, M., "A new technique for using multivariate adaptive regression splines (MARS) in pavement roughness prediction", *Proc ICE Trans*, 156(1), 51-55, 2003.

[93] Attoh-Okine, N. O., Cooger, K., Mensah, S., "Multivariate Adaptive Regression (MARS) and hinged hyperplanes (HHP) for doweled pavement performance modelling", *Constr Build Mater*, 23(9), 3020-3023, 2009.

[94] Wang, L. J., Guo, M., Sawada, K., Lin, J., and Zhang, L., "Landslide Susceptibility mapping in Mizunami city, Japan: A comparison between logistic regression, bivariate statistical analysis and multivariate adaptive regression spline models", *Journal of Catena*, 135, 271-282, 2015.

[95] Kisi, O., and Parmar, K. S. (2015), "Application of Least Square Support Vector Machine and Multivariate Adaptive Regression Spline Models in Long term Prediction of River Water Pollution", *Journal of Hydrology* , 2015, 1-28, Accessed: February 10, 2017.

[96] Samui, P. and Kim, D., "Modelling of reservoir-induced earthquakes: a multivariate adaptive regression spline", *Journal of Geophysics and Engineering*, 9, 494-497, 2012.

[97] Laurin, G. V., Puletti, N., Chen, Q., Piermaria, C., Papale, D., and Valentini, R., "Above ground biomass and tree species richness estimation with airborne Lidar in tropical Ghana forest", *International Journal of applied Earth Observation and Geoinformation*, 52, 371-379, 2016.

[98] Durmaz, M., Karslioglu, M. O., and Nohutcu, M., "Regional VTEC modelling with multivariate adaptive regression splines", *Advances in Space Research*, 46, 180-189, 2010.

[99] Durmaz, M. and Karslioglu, M. O., "Non-parametric regional VTEC modelling with Multivariate Adaptive Regression B-Splines", *Advances in Space Research*, 48, 1523-1530, 2011.

[100] Chen, M., Tompson, A. F. B., Mellors, R. S., Ramirez, A. L., Dyer, K. M., Yang, X., and Wagoner, J. L., "An efficient Bayesian inversion of a geothermal prospect using a multivariate adaptive regression spline method", *Journal of Applied Energy*, 136, 619-627, 2014.

[101] Dawod, G. M., Mirza, N. M., Al-Ghamdi, A. K., "Simple precise coordinate transformations for geomatics applications in Makkah metropolitan area, Saudi-Arabia", *Bridging the gap between cultures FIG working week*, Marrakech Morocco, 2010b, 18-22.

[102] Featherstone, W. E., "A comparison of existing co-ordinate transformation models and parameters in Australia", *Cartogr* , 26(1), 13-26, 1997.

[103] Odutola, C. A., Beiping, W., and Ziggah, Y. Y., "Testing Simple Regression Model for Coordinate Transformation by Comparing its Predictive Result for Two Regions", *Academic Research International*, SAVAP International Publishers, 4(6), 540-549, 2013.

[104] Ziggah Y. Y., "Regression Models for 2-Dimensional Cartesian Coordinates Prediction: A Case Study at University of Mines and Technology (UMaT)", *International Journal of Computer Science and Engineering Survey (ISCSES)*, 3(6), 62, 2012.

[105] Owusu, B., "An Assessment of Job Satisfaction and Its Effect on Employees' Performance: A Case of Mining Companies in the [ Bibiani- Anhwiaso – Bekwai District] in the Western Region", *A Master Thesis of Business Administration submitted to the Department of Managerial Science*, Kwame Nkrumah University of Science and Technology, Kumasi, Ghana, 108, 2014.

[106] Peprah, S. M., "Field Trip and Technical Report", *Unpublished BSc Report Notes*, University of Mines and Technology, Tarkwa, Ghana, 26, 2015.

[107] Mohammed, A. S., "Performance Assessment of the Methods used in Transformation from Cartesian Coordinates to Geodetic Coordinates", *Unpublished BSc report*, University of Mines and Technology, Tarkwa, Ghana, 65, 2015.

[108] Quarshie, E., Nyarko, B. J. B., and Serfor – Armah, Y., "Studies of the Levels of some Toxic Elements in Soil and Tailings from Bibiani Mining Area of Ghana", Research Journal of Environmental and Earth Sciences, 3(5), 512-520, 2011.

[109] Zabihi, M., Pourghasemi, H. R., Pourtjhi, Z. S., and Behzadfar, M., "GIS-based multivariate adaptive regression spline and random forest models for groundwater potential mapping in Iran", *Environ Earth Sci*, 75(665), 646-665, 2016.

[110] Petrie, G., and Kennie, T. J. M., "Terrain modelling in surveying and civil engineering", 19(4), 171-187, 1984.

[111] Miller, S. J., "Methods of Least Squares", Statistics Theory, *Cornell University*, USA, 3, 1-2, 2006.

[112] Annan, R. F., Ziggah, Y. Y., Ayer, J., and Odutola, C. A., "Accuracy Assessment of heights obtained from Total station and level instrument using Total Least Squares and Ordinary Least Squares Methods", *Journal of Geomatics and Planning*, 3(2), 87-92, 2016a.

[113] Schaffrin, B., "A note on Constrained Total Least Square estimation", Linear Algebra and Its Application, 417, 245-258, 2006.

[114] Akyilmaz, O., "Total Least Squares Solution of Coordinate Transformation", *Survey Review*, 39(303), 68-80, 2007.

[115] Golub, G. H., and Van Loan, C. F., "An analysis of the Total Least Squares problem", *SIAM Journal on Numerical Analysis*, 17(6), 883-893, 1980.

[116] Annan, R. F., Ziggah, Y. Y., Ayer, J., Odutola, C. A., "A Hybridized Centroid Technique for 3D Molodensky-Badekas Coordinate Transformation in the Ghana Reference Network using Total Least Squares Approach", *South African Journal of Geomatics*, 5(3), 269-284, 2016b.

[117] Markovsky, I., and Van Huffel, S., "Overview of Total Least Square Methods", *Signal Processing*, 87(10), 2283-2302, 2007.

[118] Okwuashi, O., and Eyoh, A., "Application of total least squares to a linear surveying network", *Journal of science and Arts*, 4(21), 401-404, 2012a.

[119] Ge, X., and Wu, J., "A New Regularized Solution to Ill-Posed Problem in Coordinate Transformation", *International Journal of Geosciences*, 3, 14-20, 2012.

[120] Okwuashi, O., and Eyoh, "3D Coordinate transformation using total least squares", *Academic Research International*, 3(1), 399-405, 2012b.

[121] Mueller, V. A., and Hemond, F. H., "Extended artificial neural networks: in-corporation of a priori chemical knowledge enables use of ion selective electrodes for in-situ measurement of ions at environmental relevant levels", *Talenta*, 117, 112-118, 2013.

[122] Yegnanarayana, B., "*Artificial neural networks*", Prentice-Hall of India Private Limited, 2005.

[123] Hornik, K., Stinchcombe, M., and White, H., "Multilayer feed forward networks are universal approximators", *Neural Netw*, 2, 359-366, 1989.

[124] Yonaba, H., Anctil, F., and Fortin, V., "Comparing sigmoid transfer functions for neural network multistep ahead stream flow forecasting", *J Hydrol Eng*, 15(4), 275-283, 2010.

[125] Konaté, A. A., Pan, H., Khan, N., and Ziggah, Y. Y., "Prediction of porosity in crystalline rocks using artificial neural networks: an example from the Chinese continental scientific drilling main hole", *Stud Geophys Geod*, 59(1), 113–136, 2015.

[126] Gope, D., Gope, P. C., Thakur, A., and Yadav, A., "Application of artificial neural network for predicting crack growth direction in multiple cracks geometry", *App Soft Comput*, 30, 514-528, 2015.

[127] Samui, P. and Kothari, D. P., "A Multivariate Adaptive Regression Spline Approach for Prediction of Maximum Shear Modulus ($G_{max}$) and Minimum Damping Ratio (£*min*), *Engineering Journal*, 16(5), 1-10, 2012.

[128] Craven, P. and Wahba, G., "Smoothing noisy data with spline function: estimating the correct degree of smoothing by the method of generalized cross-validation", *Numer Math*, 31, 317-403, 1979.